Supporting Information:

Growth and oxidation of graphene on Rh(111)

Karin Gotterbarm, Wei Zhao, Oliver Höfert, Christoph Gleichweit, Christian Papp
and Hans-Peter Steinrück

Lehrstuhl für Physikalische Chemie II, Universität Erlangen-Nürnberg, Egerlandstraße 3,

91058 Erlangen, Germany.

Fig. S1: A Rh 3d spectrum of the clean Rh(111) surface at 120 K is shown in Fig. S1 (a). The fits of the bulk contribution at 307.4 eV and the surface contribution at 306.9 eV are displayed in blue and green, respectively. In our measurements of the clean surface at 380 eV excitation energy the surface signal is as high as the bulk signal. Fig. S1 (b) shows a Rh 3d spectrum measured at 120 K after CVD of graphene. Even after the surface is saturated with carbon, the Rh 3d surface contribution has roughly half the intensity compared to the clean surface. This is a strong indication that only part of the carbon atoms of the graphene layer interact strongly with the substrate surface. Selected Rh 3d spectra measured during graphene growth are shown in Fig. S1 (c). Graphene was grown at 920 K with $2 \cdot 10^{-8}$ mbar of propene. The clean spectrum (red) is broader than in (a), due to the higher temperature. Upon propene exposure the surface contribution decreases and the bulk contribution is attenuated. The quantitative analysis of this experiment is shown in Fig. S1 (d). With increasing graphene coverage, the total Rh 3d intensity drops due to damping. In agreement with the C 1s data (see Fig. 1) the surface is saturated after an exposure to ~30 L of propene.

Table S2:. The table shows the Gaussian widths of the graphene species as well as the amount of carbidic carbon after preparation of the graphene layers in Fig. 3. These values served to quantify the quality (i.e. defect density) of the graphene layers. The Gaussian width of the C 1s contributions as well as the carbidic carbon content increase with defect density.

Fig. S3: In order to investigate the thermal stability of graphene on Rh(111) we progressively annealed a graphene layer in 50 K steps up to 1200 K. Selected Rh 3d and C 1s spectra measured at different temperatures are shown in Fig. S2 (a) and (b), respectively. Until 1050 K, the spectra (green) of both core levels do not change, except for broadening due to the higher temperature. At 1100 K (yellow spectrum) the Rh 3d surface contribution at 306.9 eV increases slightly and the C 1s signal decreases, revealing that the onset of carbon diffusion into the bulk of the crystal lies between 1050 and 1100 K. The C 1s signals of graphene and carbidic carbon decrease further upon heating to 1150 K (red spectrum) and completely vanish until 1200 K (purple spectrum). Accordingly, the surface

contribution in the Rh 3d spectra rises and is restored to almost the same intensity as the bulk contribution at 1200 K (purple spectrum). These results show that graphene layers prepared by CVD on Rh(111) are stable well up to 1000 K and can be removed effectively by diffusion of carbon into the bulk of the crystal at 1200 K. The restored Rh 3d surface contribution indicates that the surface is clean after this procedure.

Fig. S4: The full data sets for the quantitative analysis of the oxidation of high and low defect density graphene at different temperatures are displayed in Fig. S3 (a) and S3 (b), respectively. The data points denote the total graphene coverage as obtained from fitting of the two C 1s contributions. All experiments show an S-shaped time dependence and can be fitted with sigmoidal curves (dotted lines). Inspection of the data shows that e.g. at 900 K in (a) a different trend is found. Similar effects have also been obseved in additional experiments for other temperatures. This behavior is attributed to a different defect density in the layer, due to slight differences in the preparation procedure, which leads to different induction periods. In order to compare the subsequent oxidation process, the varying induction periods were accounted for by shifting each data set on the exposure axis to the exposure value corresponding to 90 percent graphene coverage; see Fig. S3 (c) and (d) for high and low defect density graphene, respectively. The resulting curves clearly show the expected monotonous increase of the reaction rate (steeper decrease of the signal) with increasing temperature.
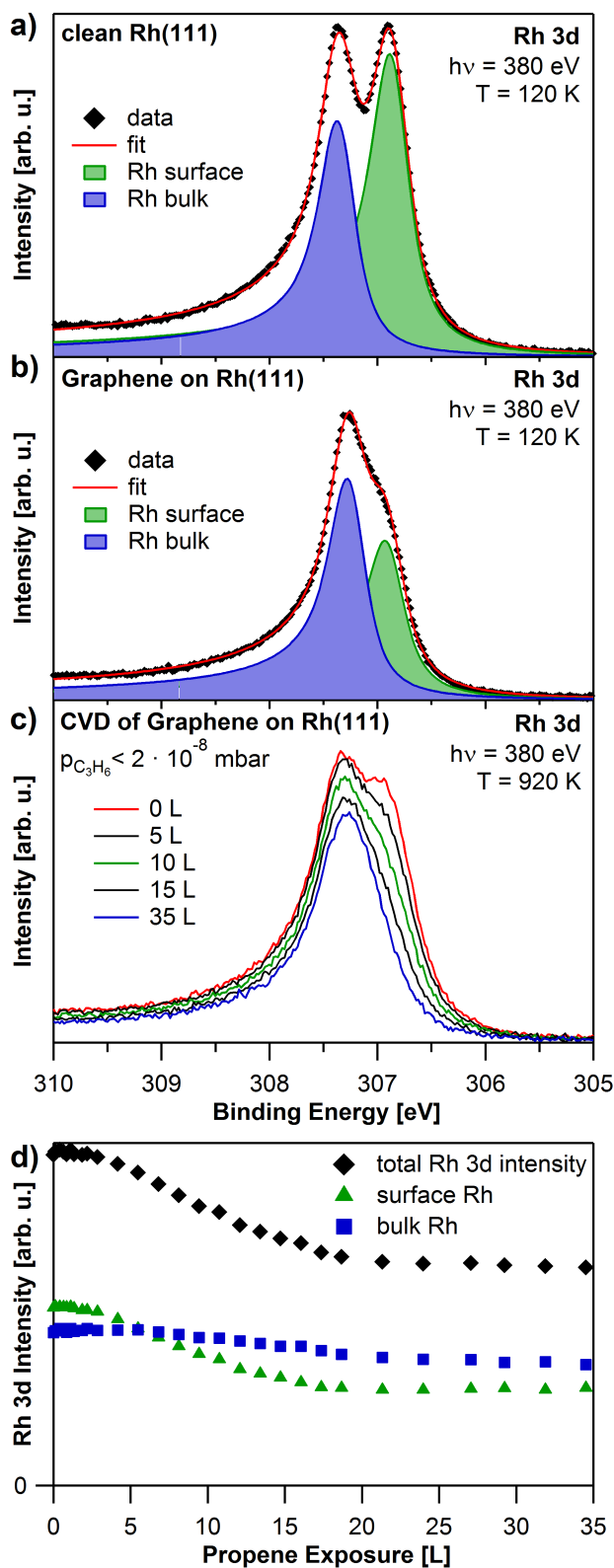
Fig. S1: *Growth of graphene on Rh(111): a) Fit of Rh 3d spectrum of the clean Rh(111) surface showing the bulk and the surface Rh contribution b) Fit of Rh 3d spectrum of graphene on Rh(111) at 120 K c) Selected Rh 3d spectra measured during graphene growth at 920 K with $2 \cdot 10^{-8}$ mbar propene pressure d) quantitative analysis of the experiment shown in b).*

Table S2: *Gaussian widths of the graphene species C_1 and C_2 and area of carbidic carbon of the spectra displayed in Fig. 3.*

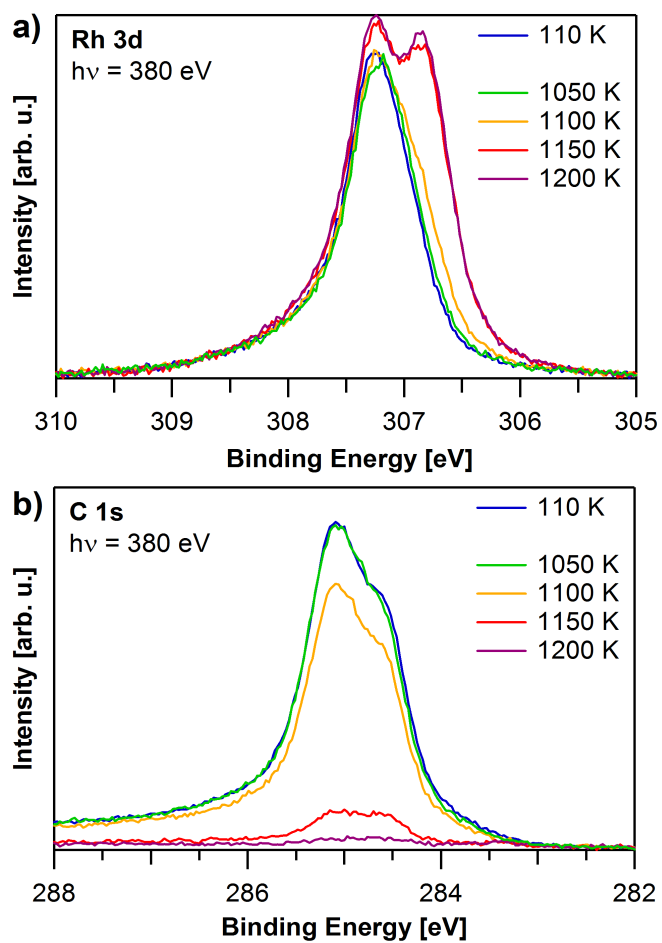|	Gaussian width (C_1)	Gaussian width (C_2)	Relative area of carbidic carbon in %
3a	0.59	0.68	6.5
3b	0.48	0.62	4.2
3c	0.35	0.25	0.0
3d	0.43	0.46	2.6
3e	0.52	0.66	4.4

Fig. S3: *Thermal stability of graphene on Rh(111): a) Selected Rh 3d spectra and b) Selected C 1s spectra measured during heating of a graphene layer.*
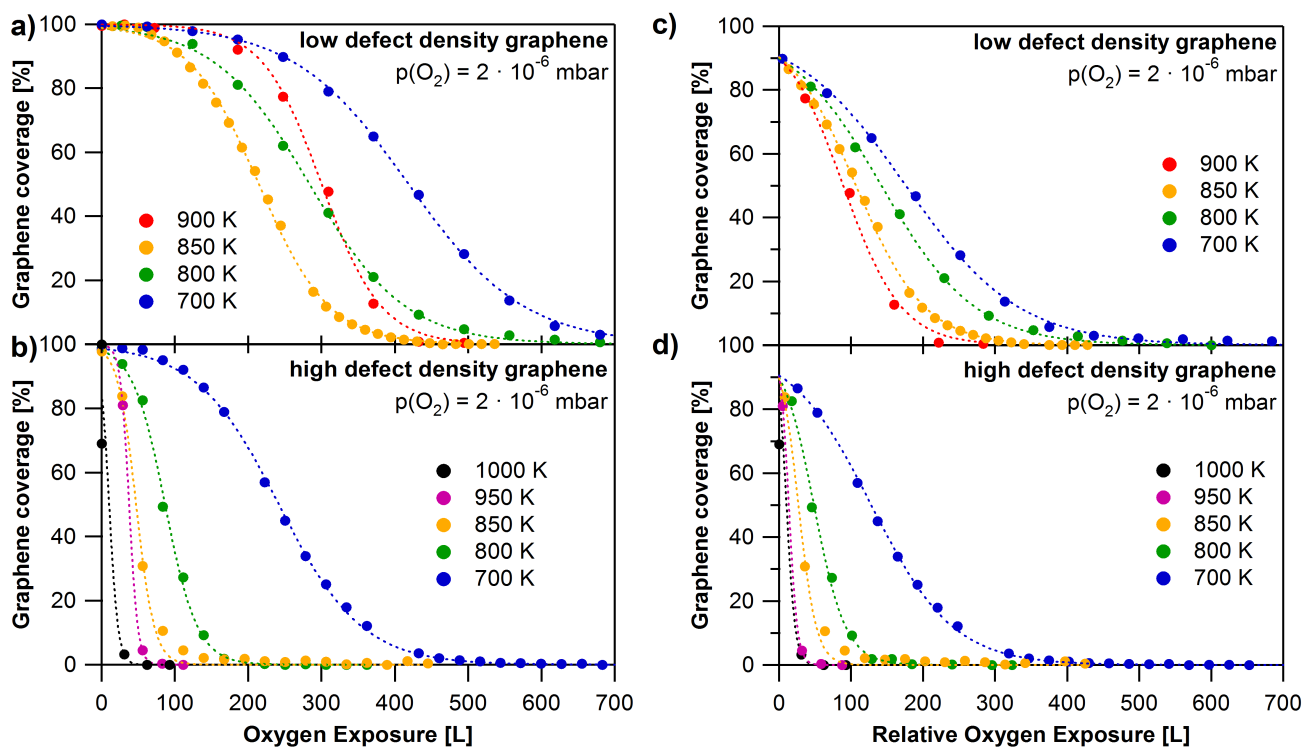
Fig. S4: *Full data set of the oxidation of graphene at $2 \cdot 10^{-6}$ mbar oxygen at temperatures between 700 and 1000 K. The data points are obtained from fitting, as the sum of both graphene C 1s contributions; dotted lines display sigmoidal fits of the data. a) low defect density graphene, b) high density graphene. In c) and d) the data sets are shifted by the exposure value corresponding to 90 percent graphene coverage, to allow a direct comparison of the reaction rates after the induction period: c) low defect density graphene: data shifted by 211.2 L (900 K); 107.7 L (850 K); 141.6 L (800 K); 242.9 L (700 K); d) high defect density graphene: data shifted 0.1 L (1000 K); 24.0 L (950 K); 20.1 L (850 K); 38.2 L (800 K); 113.7 L (700 K); respectively.*